THE ASTROPHYSICAL JOURNAL, 172:181–199, 1972 February 15

RADIAL PULSATIONS OF PRE-WHITE-DWARF STARS. I. LINEAR QUASI-ADIABATIC ANALYSIS

H. M. VAN HORN AND M. B. RICHARDSON*
Department of Physics and Astronomy and C. E. Kenneth Mees Observatory, University of Rochester

AND

CARL J. HANSEN
Joint Institute for Laboratory Astrophysics† and Department of Physics and Astrophysics, University of Colorado, Boulder

Received 1971 June 28

ABSTRACT

Numerical calculations of the periods, eigenfunctions, and stability integrals in the quasi-adiabatic limit have been carried out for the lowest radial pulsation modes of homogeneous, pre-white-dwarf stellar models. Detailed numerical results are given, and the effects of neutrino emission, differences in stellar mass, and structural changes accompanying the evolution are discussed.

I. INTRODUCTION

This paper is the first in a series dealing with the pulsational properties of stellar models in the final phases of evolution immediately prior to becoming white dwarfs. In subsequent papers of this series we shall investigate the contributions of various non-adiabatic processes to energization of the pulsations. In the present work we have studied the systematic variation with stellar mass and evolution of the properties of the lowest adiabatic, radial pulsation modes of stellar models selected from the evolutionary sequences computed by Savedoff, Van Horn, and Vila (1969, hereafter denoted by SV[2]).

The need for a comprehensive investigation of the pulsational properties of stars in the immediate pre-white-dwarf evolutionary phases has become increasingly apparent in recent years. Theoretical studies dealing with stars between the main sequence and the white dwarfs (implying radial pulsation periods ranging from several hours to some tens of seconds, respectively) have become increasingly important. Perhaps even more significant are the recent discoveries of ultrashort-period oscillations in the degenerate stars HZ 29 (P = 1051.12 s [Ostriker and Hesser 1968, and references therein]), HL Tau-76 (P = 747 s [Landolt 1968; Warner and Nather 1970]), and R548 (P = 212.86, 273 s [Lasker and Hesser 1971]), and in Nova DQ Herculis (P = 71.060 s [Walker 1961]). In addition, evidence of some quasi-periodic activities in the degenerate star G44−32 (P = 600, 822, 1638 s [Lasker and Hesser 1969]) and in the X-ray source Sco X-1 ($P \approx$ 170 s [Gribbin, Feldman, and Plageman 1970]) has been reported. These findings dramatically emphasize the pressing need to understand the pulsational attributes of stars in very late stages of evolution.

Previous work on the pulsations of highly evolved stars has dealt mainly with zero-temperature "white dwarfs." Thus, Sauvenier-Goffin (1949) and Schatzman (1961) have computed the pulsation periods of the zero-temperature models of Chandrasekhar (1939), and Ledoux and Sauvenier-Goffin (1950) have studied the stability of "warm" white-dwarf models. More recently, Meltzer and Thorne (1966) have studied the pulsations of white dwarfs composed of "cold, catalyzed matter" (Harrison *et al.* 1965), and

* Now at the State University of New York at Albany.

† Of the National Bureau of Standards and the University of Colorado.

Faulkner and Gribbin (1968) and Skilling (1968) have computed the periods of Hamada and Salpeter's (1961) cold white-dwarf models constructed with Salpeter's (1961) Coulomb-corrected equation of state. The effects of rapid rotation have been investigated by Ostriker and Tassoul (1969), and the corrections due to finite but low temperatures have been studied by Baglin (1967).

More closely related to our present work are the calculations of pulsation periods, eigenfunctions, and stability integrals for hot, partially degenerate stars that have recently been carried out by Rose and his collaborators (Rose 1967, 1968; Harper and Rose 1970). These investigations have dealt with the final phases of evolution of hydrogen- and helium-shell-burning stars just prior to the extinguishment of the nuclear energy sources. However, only a few models of mass 0.75 $M_\odot$ have been published, so that systematic variations of the pulsation properties with evolution and with stellar mass can be discussed only in a schematic fashion, if at all.

In the present work the pulsation periods, eigenfunctions, and stability integrals of the lowest few adiabatic radial pulsation modes have been computed for a substantial number of the models described by SV[2]. A brief description of the models is given in § II, together with a discussion of the effects upon our present results of the approximations used in the model construction. In § III the theoretical bases of our calculations are briefly reviewed. Our results for the periods and eigenfunctions and for the stability integrals are tabulated and discussed in § IV. We have analyzed a sufficient number of models to enable us to carry out a coarse but comprehensive study of the systematic effects of neutrino emission, evolutionary state, and variations in stellar mass upon the pulsational properties of these models. As a result we are able to discuss in some detail the characteristics of the pulsations of at least some kinds of stars on the left-hand side of the H-R diagram. (Shell-burning will of course modify these results to some extent, and we explicitly exclude discussion of such cases.) These conclusions plus a brief summary of our results are given in § V.

II. THE MODELS

The models we have analyzed in this study were selected from the evolutionary sequences of 1.0, 0.631, and 0.398 $M_\odot$ pure iron stars discussed by SV[2] (see also Vila 1965). In this work two parallel sequences of models were constructed for each choice of stellar mass—one sequence without neutrino emission processes and one which included approximate expressions for the rates of energy loss due to the pair-annihilation, photo-, and plasma-neutrino mechanisms. Structural details were given for selected models from each of these sequences. The location of the models in the H-R diagram is shown in Figure 1 (the model numbers are those of SV[2]; a suffix "N" indicates a "neutrino" model). Subsequent to the publication of that paper the 1 $M_\odot$ sequences were recomputed by using the self-consistent surface condition discussed in that work. The new sequences were identical with the original ones, except at luminosities in excess of $10^{4.3}$ $L_\odot$ in the "neutrino" sequence. In these extremely luminous models the radiation pressure gradient is comparable to the surface gravity, and the condition of hydrostatic equilibrium becomes increasingly difficult to satisfy. Models selected from these new evolutionary sequences for the present study were chosen so that the central pressures and temperatures were as close as possible to those of the models tabulated by SV[2]. For the sake of completeness, however, we have also summarized the properties of the new models in Tables 1 and 2 below, in the format of SV[2]. Model numbers in the new sequence are denoted by primes throughout.

The equation of state used in the construction of these sequences contained contributions from the iron nuclei, treated as a perfect gas, from the radiation field, and from the semirelativistic, partially degenerate, noninteracting electron gas. The actual expressions

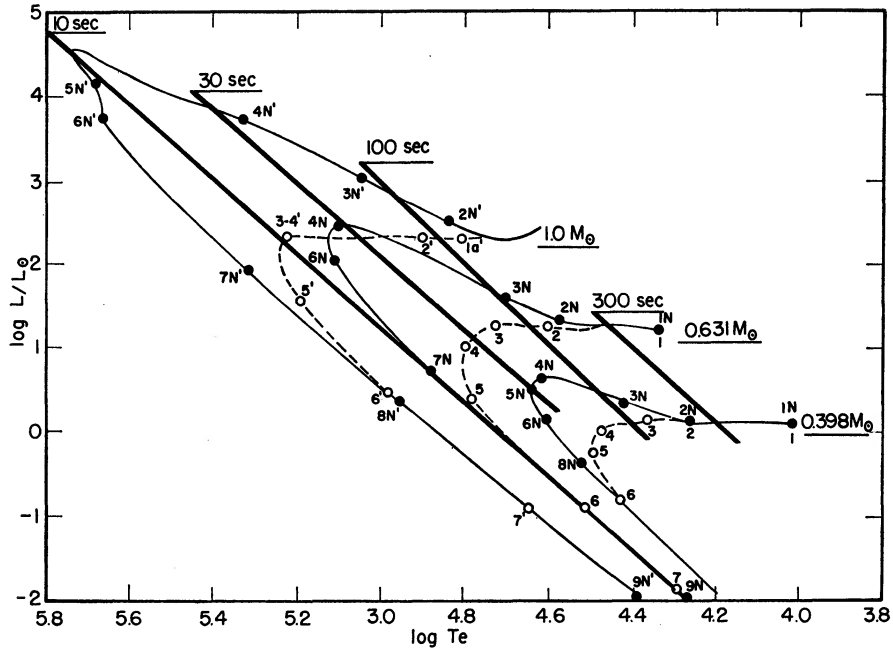

FIG. 1.—Hertzsprung-Russell diagram showing evolutionary paths of the pre–white-dwarf models without neutrino losses (*dashed curves*) and with neutrino losses (*full curves*). Lines of constant fundamental mode period are shown as heavy solid lines, with the period in seconds indicated.

TABLE 1

Properties of 1 $M_\odot$ Models Without Neutrino Loss[+]

No.	Age (years)	log ρ_c	log T_c	log P_c	ψ_c	log ρ_d	log T_d	log P_d	M_r/M	r_d/R	log $L/L_\odot$	log T_e	$R/R_\odot$
1a'	4.776 +5	4.718	8.531	20.891	-0.69	---	---	---	---	---	2.309	4.805	1.18 -1
2'	9.743 +5	5.240	8.685	21.581	+0.06	---	---	---	---	---	2.308	4.897	7.70 -2
3-4'	4.869 +6	7.113	9.089	24.095	4.91	5.136	8.633	21.439	0.952	0.581	2.317	5.224	1.73 -2
5'	1.270 +7	7.770	8.864	24.980	17.8	4.736	8.386	20.783	0.998	0.839	1.558	5.191	8.38 -3
6'	2.884 +7	7.938	8.497	25.204	49.3	4.242	8.070	19.969	1.000	0.931	0.539	4.987	6.63 -3
7'	9.374 +7	7.947	7.966	25.217	2.3 +2	3.548	7.622	18.825	1.000	0.975	-0.892	4.645	6.17 -3
8'	8.250 +8	7.948	7.152	25.217	1.5 +3	2.516	6.924	17.096	1.000	0.995	-3.033	4.116	6.00 -3
9'	4.245 +9	7.948	6.702	25.217	4.3 +3	---	---	---	---	---	-4.205	3.824	5.99 -3

[+] In all tables we use the notation 1.0 + n = 1.0 x 10^n

TABLE 2

Properties of 1 $M_\odot$ Models With Neutrino Loss

No.	Age (years)	logρ_c	logT_c	logP_c	ψ_c	$\varepsilon_{\nu,c}$	logρ_{pk}	logT_{pk}	logP_{pk}	ψ_{pk}	$\varepsilon_{\nu,pk}$	$M_{r,pk}/M$	r_{pk}/R	log$L_\nu/L_\odot$	log$L/L_\odot$	logT_e	$R/R_\odot$
2N'	3.033+5	4.906	8.497	21.054	-0.02	4.80+3	----	----	----	----	----	----	----	2.70	2.487	4.833	1.27-1
3N'	738*	6.088	8.638	22.585	+3.83	9.86+4	5.438	8.680	21.807	+0.68	1.41+5	.310	.106	4.57	3.040	5.048	8.92-2
4N'	3104*	7.339	8.502	24.369	26.2	4.58+5	5.809	8.925	22.426	+0.53	1.59+7	.767	.129	6.46	3.721	5.338	5.16-2
5N'	3633*	7.849	8.279	25.083	1.1+2	2.49+4	5.337	8.876	21.894	-0.57	6.50+6	.976	.350	5.41	4.151	5.680	1.75-2
6N'	4380*	7.906	8.204	25.161	1.3+2	4.69+3	5.388	8.794	21.855	-0.04	1.15+6	.987	.521	4.58	3.722	5.671	1.11-2
7N'	3.641+5	7.939	8.086	25.205	1.8+2	2.30+2	5.566	8.582	21.891	+1.72	2.54+4	.991	.746	2.95	1.930	5.315	7.28-3
8N'	5.076+5	7.946	7.968	25.215	2.3+2	7.73+0	5.431	8.260	21.561	+3.64	2.19+2	.996	.853	1.30	0.379	4.954	6.45-3
9N'	3.553+7	7.948	7.587	25.217	5.6+2	2.55-4	----	----	----	----	----	----	----	-1.85	-1.934	4.389	6.06-3
10N'	1.216+8	7.948	7.435	25.217	7.9+2	1.50-5	----	----	----	----	----	----	----	-3.18	-2.300	4.298	6.03-3
11N'	3.231+9	7.948	6.706	25.217	4.2+3	----	----	----	----	----	----	----	----	----	-4.194	3.826	5.99-3

* +3.500 x 10^5 years

used for the latter contribution, however, were piecewise continuous analytic formulae given explicitly by Vila (1965), which were chosen to give an accuracy of 5 percent or better in the thermodynamic functions. The adiabatic exponent $\Gamma_1 = \partial \ln P/\partial \ln \rho|_s$, which is needed throughout the pulsation calculations, is therefore given only very roughly by this equation of state, and for this reason the much more accurate values provided by interpolation in Paczyński's (1970) tables of derivatives of the thermodynamic functions were used in our final calculations of the eigenfunctions and stability integrals. For the purpose of discussing the systematic variations of the pulsations periods, however, the original equation of state is still usable: by direct comparison of the two sets of results, the periods are found to be given to ~5 percent accuracy, which is adequate for this initial survey.

III. THEORETICAL BACKGROUND

a) Adiabatic Pulsations

The general theory of small-amplitude radial pulsations and of the stability of spherically symmetric stars, in the linear approximation, has been discussed extensively by Ledoux and Walraven (1958) and more recently by Cox and Giuli (1968), whose notation we have adopted throughout this paper. For adiabatic pulsations the equation of motion for the relative pulsation amplitude,

$$\frac{\delta r(r, t)}{r} \equiv \xi(r) e^{i\sigma t},$$

becomes

$$\mathfrak{L}\xi \equiv -\frac{1}{\rho r^4}\frac{d}{dr}\left(\Gamma_1 p r^4 \frac{d\xi}{dr}\right) - \frac{1}{\rho r}\frac{d}{dr}[(3\Gamma_1 - 4)p]\xi = \sigma^2 \xi, \tag{1}$$

where p, ρ are the pressure and density of the unperturbed model. Together with the boundary conditions,

$$\frac{d\xi}{dr} = 0 \quad \text{at} \quad r = 0; \qquad \frac{d \ln \xi}{dr} = \frac{1}{\Gamma_1 R}\left[\frac{\sigma^2 R^3}{GM} - (3\Gamma_1 - 4)\right] \quad \text{at} \quad r = R \tag{2}$$

(where M, R are the stellar mass and radius, respectively), this equation constitutes the eigenvalue problem from which the eigenperiods $P_k = 2\pi/\sigma_k$ and eigenfunctions ξ_k of the adiabatic, radial pulsation modes can be determined for a given quasi-static stellar model.

Two different methods were used to solve this eigenvalue problem. The first was the variational technique, discussed by Bardeen, Thorne, and Meltzer (1966), for obtaining approximations to the eigenfrequencies σ_k of the lowest few modes. This method is based upon the fact that the eigenfrequencies are minima of the functional

$$\Sigma^2 \equiv \frac{1}{J}\int_M u^* \mathfrak{L} u r^2 dM_r; \qquad J \equiv \int_M |u|^2 r^2 dM_r, \tag{3}$$

where M_r is the mass interior to radius r, the integrals are taken over the entire star, and $u(r)$ is a function that satisfies the boundary conditions (2). Since the ξ_k satisfy the orthogonality condition

$$\int_M \xi_k^* \xi_l r^2 dM_r = J_k \delta_{kl}; \qquad J_k \equiv \int_M |\xi_k|^2 r^2 dM_r, \tag{4}$$

it follows that $\Sigma^2 = \sigma_k^2$ when $u = \xi_k$.

As our trial functions for the variational procedure we used the set of five basis functions $\{u_n: n = 0, \ldots, 4\}$ obtained from an initial set $\{r^n: n = 0, \ldots, 4\}$ or

$\{r^{2n}: n = 0, \ldots, 4\}$ by means of the Gram-Schmidt orthogonalization procedure. With this orthonormal basis set the eigenvalues of the finite-dimensional problem,

$$\left| \int_M u_n^* \mathfrak{L} u_k r^2 dM_r - \Sigma^2 \int_M |u_n|^2 r^2 dM_r \delta_{nk} \right| = 0 ,$$

are then upper bounds for the eigenfrequencies of the lowest five modes. In practice we also solved the eigenvalue problems for the lower-dimensional subspaces of our five-dimensional function space in order to assess the rate of convergence and the accuracy of the resulting approximations for σ_k. A three-dimensional function space was generally adequate to give an accuracy of a few percent in the fundamental-mode period. The five-dimensional space is in principle capable of yielding better than ~0.1 percent accuracy; however, the accuracy of the present results is limited to ~5 percent by the "noise" in the numerical values of Γ_1 derived from Vila's (1965) equation of state.

The second, and independent, method used to solve the problem was by direct integration of the two first-order differential equations in pressure and radial variations (plus boundary conditions) which are implicit in equation (1). The computational technique was embodied in a general purpose computer code given to us by N. Baker, which solves systems of first-order differential equations (with or without eigenvalues) by means of a multidimensional Newton-Raphson relaxation method. The exponent Γ_1 in these calculations was derived from Paczyński's (1970) tables. This was necessary because the pressure and radial eigenfunctions calculated were used as input for the stability analysis (to be described below) which demands accurate thermodynamic derivatives. The results of this method compare well (~5 percent error at worst) to the results of the method first described, and any errors can generally be ascribed to differences in Γ_1.

All the models considered were stable in the dynamic sense; i.e., σ^2 was positive in all cases. This is to be expected since the equation of state used restricted Γ_1 to be everywhere equal to or greater than 4/3.

b) Stability Analysis

The stability or instability of a star to radial pulsations is determined by the sign of the imaginary part κ (the reciprocal damping or growth time) of the complex pulsation frequency $\omega = \pm\sigma + i\kappa$ ($\kappa > 0$ implies stability). The calculation of κ necessarily requires the treatment of the nonadiabatic terms in the equation of motion. If these terms are small (as is always the case in our calculations), the conventional quasi-adiabatic analysis gives (see, e.g., Cox and Giuli 1968)

$$\kappa \approx -\frac{C_r}{2J\sigma^2}; \quad C_r \equiv \int_M (\Gamma_3 - 1)\frac{\delta\rho}{\rho}\delta\left(\epsilon - \frac{dL_r}{dM_r}\right) dM_r , \tag{5}$$

where J is defined in equation (4), ϵ is the *net* rate of energy generation (nuclear minus neutrino), and the δ-variation refers only to spatial changes, computed using the (real) adiabatic pulsation eigenfunction. Since C_r is evidently proportional to the luminosity L (and hence $\kappa \propto t_K^{-1}$, where t_K is the Kelvin time) the quantity we tabulate is the ratio C_r/L.

The integrations indicated in equation (5) were carried out in our calculations only to that point (the "transition zone") in the envelope of the model where nonadiabatic effects begin to become important for stability. This is acceptable here because the mass above the transition zone comprises a negligible fraction of the total stellar mass in these hot objects and thus contributes little to the integral (see chap. 27 of Cox and Giuli 1968).

In the analysis leading up to equation (5) the implicit assumption has been made

that the zero-order rate of entropy change, $T\partial s/\partial t = \epsilon - \partial L_r/\partial M_r$, is negligible. While this is emphatically not the case in the models we have studied, we shall defer discussion of this problem to the second paper of this series (Van Horn, Cox, and Hansen 1971). Preliminary indications are that while the additional contributions to the stability integral due to "thermal imbalance" (i.e., to the fact that $\epsilon - \partial L_r/\partial M_r \neq 0$) are small for the nondegenerate models, they may compensate for an appreciable fraction of the damping in cases of extreme degeneracy.

IV. NUMERICAL RESULTS

The results of our numerical calculations are summarized in Tables 3–10 and in Figures 1–7. For the unperturbed models we have listed the luminosity L, the mean density $\langle\rho\rangle$,[1] the degree of central condensation as measured by the ratio $\rho_c/\langle\rho\rangle$ of central to mean density, and the e-folding time $(d \ln T_c/dt)^{-1}$ for the central temperature. The pulsation properties tabulated include the period P_0 of the fundamental mode, the ratio P_1/P_0 of the first-harmonic to the fundamental-mode periods, and the dimensionless pulsation "constant" $Q^* \equiv P_0(G\langle\rho\rangle)^{1/2}$ all derived from our variational computations. In those cases for which we have also obtained the exact eigenfunctions and eigenvalues the differences in the values of P_0 calculated by the two methods are in all cases less than 5 percent and in most cases less than 3 percent; these differences arise from "noise" in the equation of state used in the variational calculations. For selected models we have also tabulated the exact fundamental-mode eigenfunctions $\xi_r \equiv \delta r/r$ and $\xi_P \equiv \delta p/p$ at the center (0) and the surface (R), the damping integrals C_r/L, and the imaginary part κ of the complex pulsation frequency. In all cases we take $\xi_r = 1$ at the stellar surface.

a) Comparison with Previous Work

In Table 9 and Figure 2 we have compared our results with those obtained previously by other investigators. The fundamental-mode periods and the period ratios of the

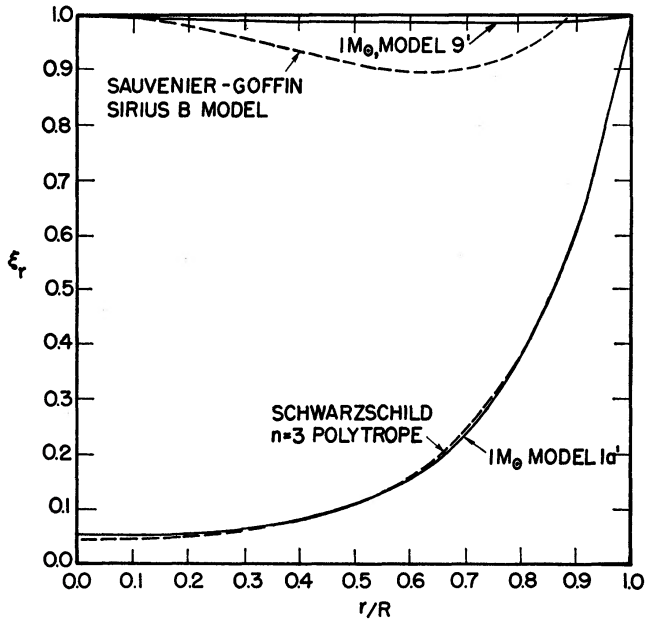

FIG. 2.—Radial eigenfunctions ξ_r versus fractional radius r/R for extremely degenerate and extremely nondegenerate models. *Full curves*, models from this paper. Note that Sauvenier-Goffin's eigenfunction is normalized to unity at $r = 0$.

[1] *Note added in proof.*—In the tables and figures $\langle\rho\rangle$ is denoted by $\bar{\rho}$.

TABLE 3

Pulsation Properties of 1 $M_\odot$ Models With Neutrino Loss

No.	log $L/L_\odot$	log $\bar{\rho}$	$\rho_c/\bar{\rho}$	$(d\ln T_c/dt)^{-1}$ years	P_0(sec)	P_1/P_0	Q*	$\xi_r(0)$	$\xi_p(0)$	$\xi_p(R)$	C_r/L	κ^{-1}(yrs)
2N'	2.487	2.833	118.3	3.9 +5	152.	.75	1.02	----	----	----	----	----
3N'	3.040	3.274	651.6	4.1 +4	88.5	.70	.99	----	----	----	----	----
4N'	3.721	4.012	2123.	-1.0 +3	38.3	.70	1.00	6.29 -4	-2.69 -3	-14.2	-77.	.60
5N'	4.151	5.422	267.3	-2.6 +3	8.16	.65	1.08	----	----	----	----	----
6N'	3.722	6.016	77.63	-6.3 +3	4.68	.73	1.23	.214	-.884	-10.1	-49.	4.8 +2
7N'	1.930	6.562	23.82	-6.4 +4	4.47	.39	2.20	----	----	----	----	----
8N'	0.379	6.721	16.79	-5.5 +5	4.41	.35	2.61	----	----	----	----	----
9N'	-1.934	6.802	14.00	-3. +7	4.40	.34	2.86	.993	-4.10	-5.09	-38.	5.7 +9
10N'	-2.300	6.808	13.80	-1. +8	4.40	.34	2.88	----	----	----	----	----
11N'	-4.194	6.817	13.52	-1. +9	4.40	.34	2.91	.995	-4.11	-5.05	-12.	3.3 +12

TABLE 4

Pulsation Properties of 1 $M_\odot$ Models Without Neutrino Loss

No.	log $L/L_\odot$	log $\bar{\rho}$	$\rho_c/\bar{\rho}$	$(d\ln T_c/dt)^{-1}$ years	P_0(sec)	P_1/P_0	Q*	$\xi_r(0)$	$\xi_p(0)$	$\xi_p(R)$	C_r/L	κ^{-1}(yrs.)
1a'	2.309	2.935	60.67	1.2 +6	142.	.74	1.08	5.24 -2	-.244	-12.9	-60.	4.5 +2
2'	2.308	3.490	56.23	1.5 +6	78.1	.72	1.12	----	----	----	----	----
3'	2.314	4.483	48.64	4.0 +6	26.9	.67	1.21	----	----	----	----	----
4'	2.317	5.437	47.42	-1.2 +8	10.3	.60	1.39	.306	-1.32	-8.91	-27.	5.6 +4
5'	1.558	6.379	24.60	-1.1 +7	4.92	.44	1.97	----	----	----	----	----
6'	0.539	6.685	17.91	-1.4 +7	4.45	.36	2.53	----	----	----	----	----
7'	-0.892	6.778	14.76	-5. +7	4.41	.34	2.79	.986	-4.07	-5.15	-11.	1.7 +9
8'	-3.033	6.814	13.61	-3. +8	4.40	.34	2.90	----	----	----	----	----
9'	-4.205	6.817	13.52	-8. +8	4.40	.34	2.91	.995	-4.11	-5.05	-12.	3.3 +12

TABLE 5

Pulsation Properties of 0.631 $M_\odot$ Models With Neutrino Loss

No.	log $L/L_\odot$	log $\bar{\rho}$	$\rho_c/\bar{\rho}$	$(d\ln T_c/dt)^{-1}$ years	P_0(sec)	P_1/P_0	Q*	$\xi_r(0)$	$\xi_p(0)$	$\xi_p(R)$	C_r/L	κ^{-1}(yrs.)
1N	1.226	1.574	77.63	4. +5	612	.72	.97	2.11 -2	-.102	-14.6	-69	4.0 +2
1Na	1.273	1.988	70.15	3.0 +6	382	.72	.97	----	----	----	----	----
2Na	1.327	2.825	70.31	4.0 +6	152	.71	1.02	----	----	----	----	----
3N	1.602	3.182	135.2	-3.0 +6	96.9	.71	.98	----	----	----	----	----
3Na	2.246	3.773	277.3	-1.1 +5	46.1	.67	.92	----	----	----	----	----
4N	2.434	4.337	184.5	-1.2 +5	24.6	.71	.94	5.01 -3	-2.25 -2	-15.2	-73.	3.5 +1
6N	2.037	4.994	63.97	-2.3 +5	13.0	.76	1.06	5.24 -2	-.232	-13.2	-59.	1.3 +3
6Na	1.578	5.276	37.67	-4.9 +5	11.2	.66	1.25	----	----	----	----	----
7N	0.725	5.570	21.14	-1.9 +6	10.0	.52	1.58	----	----	----	----	----
9N	-1.970	5.900	10.42	-3. +7	9.66	.39	2.22	.798	-3.50	-6.09	-94.	8.9 +8
10N	-2.780	5.927	9.795	-3. +8	9.66	.39	2.29	----	----	----	----	----
11N	-4.228	5.945	9.397	-1.5 +9	9.66	.39	2.34	.824	-3.61	-5.88	-21.	7.6 +11

TABLE 6

Pulsation Properties of 0.631 $M_\odot$ Models Without Neutrino Loss

No.	log $L/L_\odot$	log $\bar{\rho}$	$\rho_c/\bar{\rho}$	$(d\ln T_c/dt)^{-1}$ years	P_0(sec)	P_1/P_2	Q*	$\xi_r(0)$	$\xi_p(0)$	$\xi_p(R)$	C_r/L	κ^{-1}(yrs.)
1	1.226	1.574	77.63	4. +5	610	.72	.97	2.11 -2	-.102	-14.6	-64.	4.0 +2
1a	1.271	1.985	70.15	3. +6	383	.72	.97	----	----	----	----	----
1b	1.267	2.309	62.23	4. +6	271	.71	1.00	----	----	----	----	----
2	1.253	3.332	53.21	7.2 +6	90.0	.68	1.08	----	----	----	----	----
3	1.261	3.833	48.87	1.8 +7	50.6	.65	1.08	----	----	----	----	----
4	1.001	4.649	33.88	-1.4 +8	22.7	.65	1.24	.233	-1.06	-10.1	-31.	2.4 +5
5	0.378	5.474	20.94	-4.5 +7	11.6	.51	1.63	----	----	----	----	----
6	-0.910	5.819	12.42	-8.1 +7	9.74	.41	2.04	----	----	----	----	----
7	-1.857	5.894	10.57	-1.4 +8	9.66	.39	2.21	.793	-3.48	-6.12	-18.	3.6 +9
8	-2.494	5.918	10.00	-3. +8	9.66	.39	2.27	----	----	----	----	----
9	-3.678	5.942	9.462	-7. +8	9.66	.39	2.33	.821	-3.60	-5.91	-20.	2.3 +11

TABLE 7

Pulsation Properties of 0.398 $M_\odot$ Models With Neutrino Loss

No.	log $L/L_\odot$	log $\bar{\rho}$	$\rho_c/\bar{\rho}$	$(d\ln T_c/dt)^{-1}$	P_0(sec)	P_1/P_2	Q*	$\xi_r(0)$	$\xi_p(0)$	$\xi_p(R)$	C_r/L	κ^{-1}(yrs.)
1N	0.105	1.101	72.95	1.5 +5	1036	.72	.93	1.99 -2	-9.81 -2	-14.9	-65.	1.7 +3
1Na	0.154	1.671	64.42	1.8 +7	540	.72	.95	----	----	----	----	----
1Nb	0.143	2.070	57.41	2.1 +7	348	.71	.97	----	----	----	----	----
2Na	0.189	2.808	61.38	2.6 +7	152	.68	1.00	----	----	----	----	----
3N	0.347	3.168	79.25	-3.2 +7	100	.72	.99	----	----	----	----	----
4N	0.647	3.924	84.53	-3.0 +6	40.8	.71	.97	2.28 -2	-.108	-14.4	-62.	4.8 +3
5N	0.544	4.224	57.28	-4.5 +6	29.9	.74	1.00	----	----	----	----	----
6N	0.121	4.617	29.79	-1.1 +7	21.0	.71	1.10	.150	-.700	-11.4	-42.	3.4 +5
8N	-0.391	4.866	18.84	-4.1 +7	18.2	.63	1.28	----	----	----	----	----
9N	-2.117	5.220	9.120	-1.0 +8	16.8	.46	1.77	.665	-3.09	-6.91	-64.	5.3 +8
10N	-3.057	5.286	7.834	-3. +8	16.7	.44	1.90	----	----	----	----	----
11N	-4.132	5.322	7.244	-2. +9	16.7	.44	1.98	.742	-3.45	-6.33	-24.	1.8 +11

TABLE 8

Pulsation Properties of 0.398 $M_\odot$ Models Without Neutrino Loss

No.	log $L/L_\odot$	log $\bar{\rho}$	$\rho_c/\bar{\rho}$	$(d\ln T_c/dt)^{-1}$ years	P_0(sec)	P_1/P_2	Q*	$\xi_r(0)$	$\xi_p(0)$	$\xi_p(R)$	C_r/L	κ^{-1}(yrs.)
1	0.105	1.101	72.95	1.5 +5	1036	.72	.93	1.99 -2	-9.81 -2	-14.9	-65.	1.7 +3
1a	0.154	1.671	64.42	1.8 +7	536	.72	.95	----	----	----	----	----
1b	0.142	2.070	57.02	2.2 +7	346	.72	.97	----	----	----	----	----
2	0.135	2.643	53.33	2.9 +7	185	.70	1.00	----	----	----	----	----
3	0.154	3.081	54.33	3.7 +7	115	.69	1.03	----	----	----	----	----
4	0.017	4.008	37.41	-2.6 +8	42.4	.69	1.11	.122	-.574	-11.8	-41.	2.3 +5
5	-0.167	4.407	28.05	-1.5 +8	27.6	.68	1.14	----	----	----	----	----
6	-0.799	4.899	15.81	-1.7 +8	18.8	.58	1.37	----	----	----	----	----
7	-2.105	5.214	9.226	-3.6 +8	16.8	.46	1.76	.661	-3.07	-6.91	-20.	1.6 +9
9	-3.923	5.316	7.345	-1.2 +9	16.8	.44	1.97	.739	-3.43	-6.35	-23.	1.1 +11

TABLE 9

Comparisons With Previous Calculations

A. White Dwarf Models

	This paper						Schatzman (1961)			Meltzer & Thorne (1966)			Harper & Rose (1970)		
$\log \rho_c$	$M/M_\odot$	No.	$\log L/L_\odot$	ψ_c	P_0	P_1/P_0	P_2/P_1	P_0	P_1/P_0	P_2/P_1	P_0	P_1/P_0	P_2/P_1	P_0	P_1/P_0	P_2/P_1
7.948	1.0	9'	-4.205	4.3 +3	4.40	0.34	0.66	4.56	---	---	9.65*	.19*	.65	4.62	.34	.66
6.918	0.631	11N	-4.228	1. +3	9.66	0.39	0.68	9.08	---	---	8.84	.40	.67	9.43	.41	.67
6.182	0.398	11N	-4.132	320	16.7	0.44	0.68	17.0	---	---	16.2	.43	.66	18.5	.43	.67

* Affected by differences in equation of state: see text.

B. Non-Degenerate Models

$M/M_\odot$	No.	ψ_c	$\rho_c/\bar{\rho}$	Q^*	P_1/P_0
1.0	1a'	-0.69	60.67	1.08	0.74
0.631	1N	-1.80	77.63	0.97	0.72
0.398	1N	-1.94	72.95	0.93	0.72
n = 3 polytrope **			54.2	0.99	0.738

** Schwarzschild (1941)

C. Intermediate Models

$M/M_\odot$	$\log \bar{\rho}$	No.	P_0	$\xi_p(R)$	κ^{-1}(yrs.)
	2.935	1a'	142	-12.9	4.5 +2
1.0	4.483	3'	26.9	---	---
	5.437	4'	10.3	-8.91	5.6 +4
	2.31	3C+	276	-22	3. -1
0.75	4.35	3B+	33	-12	7. +3
	4.85	3D+	18	-13	7. +4
	1.574	1	610	-14.6	4.0 +2
0.631	2.309	---	271	---	---
	4.649	4	22.7	-10.1	2.4 +5

+ H_e shell-burning models by Rose (1967)

TABLE 10

First Harmonic Properties of 0.398 $M_\odot$ Models With Neutrino Loss

No.	$\xi_r(0)$	$\xi_p(0)$	$\xi_p(R)$	$\frac{r}{R}(\xi_r=0)$	$\frac{r}{R}(\xi_p=0)$	c_r/L	κ^{-1}(yrs.)
1N	-8.38 -3	+4.12 -2	-22.6	0.67_6	0.59_0	-156	83
4N	-8.75 -3	+4.15 -2	-22.3	0.67_2	0.58_7	-153	210
6N	-2.28 -2	+.107	-19.3	0.60_3	0.50_9	-117	6.5 +3
9N	-.116	+.537	-18.4	0.65_0	0.52_8	-137	2.1 +7
11N	-.248	+1.15	-16.5	0.68_8	0.55_6	-318	3.7 +9

lowest few radial pulsation modes of a number of white-dwarf models are listed in section A of the table. In addition to our results for the most strongly degenerate pure iron models computed by SV[2], we have also tabulated the results of Schatzman (1961) and of Harper and Rose (1970) for Chandrasekhar's (1939) zero-temperature models and the results obtained by Meltzer and Thorne (1966) for models consisting of "cold catalyzed matter" (CCM). In order to make a direct comparison among these calculations, we have scaled the densities and periods obtained by Schatzman and by Harper and Rose to the values appropriate for a mean molecular weight per electron $\mu_e = A/Z = 56/26 = 2.15$ and have then interpolated in the corresponding tables to obtain

the results at the same central densities as the SV[2] models. In the case of Meltzer and Thorne's calculations, we have interpolated directly in log ρ_c to obtain the results attributed to them. This provides no difficulties in the lower-mass stars, since CCM is identical with iron at low densities. For the more massive stars, however, electron captures at the correspondingly higher densities increase the value of μ_e significantly above 2.15, so that the pulsation properties of these models are no longer comparable with our results.

It is illuminating also to undertake a comparison of the eigenfunctions for degenerate stars. In Figure 2 we exhibit the result of our calculation for the radial eigenfunction ξ_r of the 1 $M_\odot$, no-neutrino model 9′, together with the result obtained by Sauvenier-Goffin (1949) for a zero-temperature model of Sirius B ($M \approx 1\ M_\odot$). Although the eigenfunctions agree to within the combined inaccuracies of our calculation plus that of Sauvenier-Goffin's variational technique, it would be interesting to know whether or not the curious dip appearing in Sauvenier-Goffin's ξ_r is real. In our calculations using the Paczyński equation of state (shown here) it does not appear. In earlier calculations using the piecewise continuous equation of state due to Vila (1965) we had found the form of ξ_r to be strikingly similar to that obtained by Sauvenier-Goffin; but "noise" in the values of Γ_1 obtained from this equation of state make these results highly suspect. An analogous, but less pronounced, structure also appears in the models with $\rho_c \approx 10^7$ g cm^{-3} studied by Meltzer and Thorne; however, in their calculations, differences between the equation of state of CCM and that of normal white-dwarf matter begin to be important in just this density range, and this may account for the differences between their results and ours. Evidently the form of the radial eigenfunction depends rather sensitively upon the equation of state, and within the accuracy of our present results we cannot determine whether or not ξ_r actually should exhibit a minimum between the center and the surface.

In section B of Table 9 we have tabulated some of the properties of our least degenerate models, together with the corresponding results obtained by Schwarzschild (1941) for a polytrope of index $n = 3$. The radial eigenfunction for the 1 $M_\odot$, no-neutrino model 1a′ is also plotted—in Figure 2—along with Schwarzschild's results for ξ_r. On the scale of this figure the two are indistinguishable. Since these early models are quite nondegenerate even at the center (as indicated by the fact that the degeneracy parameter at the center is $\psi_c < 0$), and since both the opacity and the rate of gravitational energy generation are relatively slowly varying throughout these models (see SV[2]), one would *a priori* expect the standard model to provide quite a good approximation for the run of temperature and density in these stars. It is thus perhaps not surprising that the pulsational properties also should be well approximated by those of the standard model.

Finally, in section C of the table we have compared some calculations by Rose (1967) for shell-burning stars near the peak of a "thermal pulse" with some of our intermediate models having similar masses and mean densities. Rose's models also resemble ours in the additional sense that radiative losses and nuclear burnings do not balance, although in some of his models the rate of nuclear energy production far exceeds the optical luminosity of the star. It is noteworthy that in spite of the rather extreme physical differences between the two sets of models, not only are the pulsation periods similar for similar mean densities, but even the eigenfunctions ξ_p and the radiative damping times κ^{-1} (=Rose's $-2/I_L$) are also comparable. (Note that we are comparing only the radiative damping integrals and not the complete stability integrals; Rose's model 3B is in fact pulsationally unstable due to the nuclear driving.) The exception in this comparison is with Rose's model 3C, for which he obtains a much shorter damping time than we would have expected on the basis of our calculations. The explanation of this difference lies in the extremely rapid decline of the eigenfunction toward the interior of the star; Rose obtains $\xi_r = 3.1 \times 10^{-5}$ at $M_r/M = 0.949$, while even at the centers

of our models ξ_r has only fallen to $\sim(2\text{–}5) \times 10^{-2}$. The rapid drop in ξ_r is apparently due to the fact that this particular model has a distended envelope, and this acts strongly to decrease $\xi_r^{(0)}$. Because of the fact that the pulsational properties of a star do depend upon $\rho_c/\langle\rho\rangle$ (see below), and because $\rho_c/\langle\rho\rangle$ has a much wider possible range of variation in heterogeneous stars (such as shell-burning stars), it is clear that our calculations will not accurately represent all of the pulsation properties of stars below the main sequence. Nevertheless, the fact that our results approximate the eigenfunctions and damping integrals of more complex models as well as they do may make them useful in other studies of the pulsation properties of stars in these late evolutionary phases.

b) Fundamental-Mode Periods

The large decrease in the period of the fundamental mode during evolution of a star to the white-dwarf stage, which is apparent in Tables 3–8, is a result of the enormous increase in the mean density. This effect is embodied in the well-known relation $P_0 \propto (G\langle\rho\rangle)^{-1/2}$, which follows simply from a dimensional analysis of the eigenvalue equation (3). The dimensionless pulsation "constant" Q^*, defined by[2]

$$Q^* \equiv P_0(G\langle\rho\rangle)^{1/2}\,, \tag{6}$$

is thus almost constant throughout the evolution of the star. This expected near-constancy is borne out by our calculations (Tables 3–8). There is, however, a systematic variation of Q^* during the evolution, as shown in Figure 3, which is evidently connected with the systematic structural readjustments of the star as it contracts to higher densities and becomes increasingly degenerate.

A qualitative understanding of the effects upon Q^* of these changes in the stellar structure can be obtained from the work of Ledoux and Pekeris (1941). These investigators showed that a better approximation for the fundamental-mode eigenfrequency than that given simply by the dimensional analysis is

$$\sigma_0^2 \approx (3\langle\Gamma_1\rangle - 4)(-\Omega/I)\,, \tag{7}$$

where

$$\Omega = -\int_0^R \frac{GM_r dM_r}{r}\,, \qquad I = \int_0^R r^2 dM_r\,, \tag{8}$$

and the average value of Γ_1 is defined by

$$\langle\Gamma_1\rangle \equiv \int_0^R \Gamma_1 p dV \Big/ \int_0^R p dV\,. \tag{9}$$

From the definition (6) the approximate value of Q^* can thus be found for any given density distribution.

To investigate the effects of variations in $\rho_c/\langle\rho\rangle$ upon Q^* we have taken a particularly simple distribution,

$$\rho(r) = \rho_c[1 - (r/R)^\alpha]\,, \tag{10}$$

for which the degree of central condensation is given by

$$\frac{\rho_c}{\langle\rho\rangle} = \frac{3+\alpha}{\alpha}\,. \tag{11}$$

[2] Note that our dimensionless quantity Q^* is related to the conventional pulsation constant, $Q \equiv P_c(\langle\rho\rangle/\langle\rho_\odot\rangle)^{1/2}$, by the factor $Q/Q^* = (G\langle\rho_\odot\rangle)^{-1/2} = 0^d.0379$.

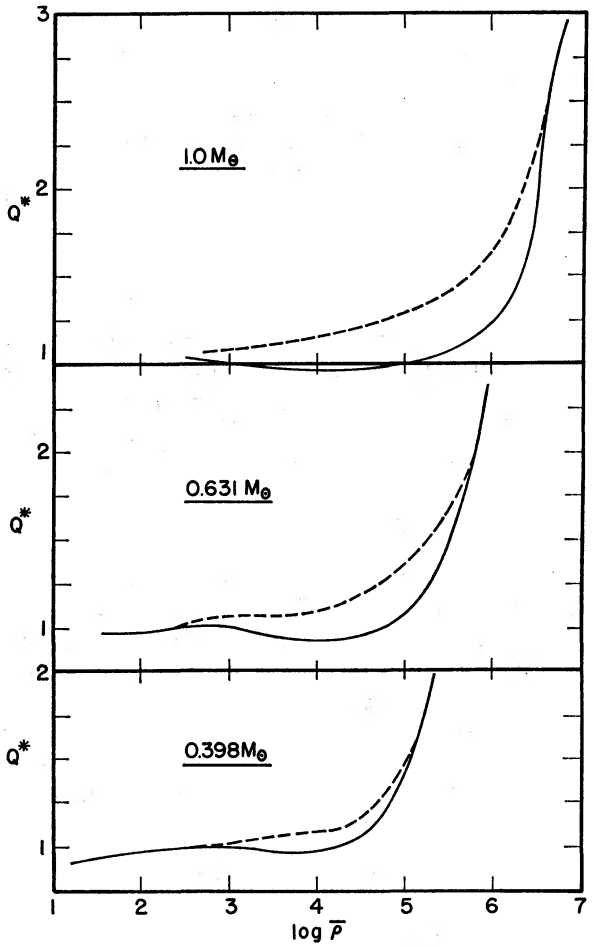

FIG. 3.—Variation with stellar mass and mean density of the dimensionless pulsation constant Q^* defined by eq. (6) for both neutrino (*full curves*) and no-neutrino (*dashed curves*) models. Note $Q^* < 1$ for some of the 1 $M_\odot$ neutrino models.

The pulsation constant then becomes

$$(Q^*)^2 = \frac{\pi}{\langle \Gamma_1 \rangle - 4/3} \frac{5(\rho_c/\langle \rho \rangle) + 1}{11(\rho_c/\langle \rho \rangle) - 5}. \tag{12}$$

This simple model indicates that Q^* becomes independent of $\rho_c/\langle \rho \rangle$ when $\rho_c/\langle \rho \rangle$ becomes large (for this model, variations are less than 10 percent when $\rho_c/\langle \rho \rangle \gtrsim 7$); while for "small" $\rho_c/\langle \rho \rangle$, Q^* increases as $\rho_c/\langle \rho \rangle$ decreases. These results reflect the fact that, as the degree of central concentration is decreased, the mass is distributed more evenly, with more of the mass at larger fractional radii; hence I/MR^2 is decreased and $|\Omega|/(GM^2/R)$ is decreased, resulting in the observed increase in Q^*.

The approximate independence of Q^* and $\rho_c/\langle \rho \rangle$ in the limit of $\rho_c/\langle \rho \rangle$ large provides the explanation for the difference in behavior of Q^* versus $\langle \rho \rangle$, shown in Figure 3, for the models with and without neutrino emission. For given $\langle \rho \rangle$, $\rho_c/\langle \rho \rangle$ is appreciably larger in the neutrino models because of the rapid core contraction; consequently, Q^* remains almost constant to larger values of $\langle \rho \rangle$ than for the no-neutrino models. The same effect explains the interesting result, depicted graphically in Figure 1, that neutrino emission has no appreciable influence upon the location in the H-R diagram of the constant-

period lines for these early phases of evolution; with Q^* fixed, constant period implies constant $\langle\rho\rangle$ and thus, for a given mass,[3] constant radius.

The increase in Q^* as the stars evolve into degenerate white dwarfs, as exhibited in Tables 3–8 and Figure 3, can also be understood on the basis of equation (12). As the density of such a star increases, the degenerate electrons become relativistic, so that $\langle\Gamma_1\rangle$ decreases from the value 5/3 appropriate to a nonrelativistic gas toward the value 4/3 which holds for the extreme-relativistic case, and Q^* is increased appreciably. This variation in $\langle\Gamma_1\rangle$ dominates in the more massive stars, and provides the explanation for the increase of Q^* with stellar mass in our most strongly degenerate models. The same result was of course already implicit in the work of Schatzman (1961), who found for white dwarfs of $\mu_e = 2$ that Q^* increased from a value of 1.91 at 0.220 $M_\odot$ to a value of 5.06 at 1.375 $M_\odot$.

c) *Fundamental-Mode Eigenfunctions*

The eigenfunctions $\xi_r \equiv \delta r/r$ and $\xi_p \equiv \delta p/p$ for the fundamental mode of pulsation are shown in Figure 4 for a selection of our models both with and without neutrino losses. In all cases we find that ξ_r decreases monotonically inward; i.e., there are no relative minima as in Sauvenier-Goffin's (1949) variational eigenfunction (Fig. 2).

The changes in the eigenfunctions during evolution can be qualitatively understood on the basis of the variations of Q^* discussed above and are apparently governed mainly by the surface boundary condition, equation (2). This relation fixes the e-folding distance H_R of ξ_r at the stellar surface. In terms of Q^*, equation (2) can be rewritten as

$$\frac{H_R}{R} = \frac{\Gamma_1 (Q^*)^2}{3\pi - (3\Gamma_1 - 4)(Q^*)^2} \cdot \tag{13}$$

As the star becomes increasingly degenerate (and ultimately relativistically degenerate) Q^* increases, and ξ_r consequently decreases inward more slowly. Thus for nondegenerate models, where $Q^* \approx 1$ and $\Gamma_1 \approx 5/3$, we expect $H_R/R \approx 0.2$, in qualitative agreement with our numerical results shown in Figure 4. For the degenerate stars H_R/R must be estimated separately for the different stellar masses. In the 0.398 $M_\odot$ models $\langle\Gamma_1\rangle \approx 5/3$, and this, together with the relatively small value of $\rho_c/\langle\rho\rangle$, leads to correspondingly small Q^* (=1.98 from our numerical calculations), giving $H_R/R \sim 1.2$; ξ_r thus decreases inward quite slowly, remaining large even in the deep interior of the star. For the 1.0 $M_\odot$ stars $\langle\Gamma_1\rangle$ approaches 4/3, which leads to larger $\rho_c/\langle\rho\rangle$ (=13.52 from the numerical models) and, from equation (12), to $(Q^*)^2\,(\Gamma_1 - 4/3) \approx 1.5$, giving $H_R/R \sim 2.3$. The pulsation amplitude thus decreases inward even less rapidly for the more massive stars, which explains the result, shown by our numerical work, that $\xi_r^{(0)}$ increases with the total stellar mass for these degenerate configurations.

d) *Harmonic Pulsations*

The results of our variational calculations for the ratio P_1/P_0 of first-harmonic to fundamental-mode periods are listed in Tables 3–8 and are also shown graphically in Figure 5 as functions of the mean densities of the stars. We have also computed the exact eigenfunctions and damping integrals for the first-harmonic mode, but only for a few models from the 0.398 $M_\odot$ neutrino-emission sequence. These results are summarized in Table 10, and the radial eigenfunctions ξ_r for these models are depicted in Figure 6. In addition, we have variational estimates for periods of a few higher modes, but the

[3] The effect upon the P = constant lines of differences in the stellar mass is also effectively negligible, as can be seen by the following homology argument: For $\langle\rho\rangle$ = constant, $R \propto M^{1/3}$, and the temperature $T \propto GM\mu H/kR \propto M^{2/3}$. The temperature gradient equation with a generalized Kramers's law opacity, $K = K_0\rho^n T^{-s}$ then gives $L \propto M^{(9+2s)/3}$. From Stefan's law $L \propto R^2 T_e^4 \propto M^{2/3} T_e^4 \propto L^{2/(9+2s)} T_e^4$ we thus obtain $d \log T_e/d \log L = \frac{1}{4}[1 - 2/(9 + 2s)]$. For Kramers's law, $s = 3.5$, giving a fractional difference from the slope of the lines R = constant of $-2/(9 + 2s) = -0.125$; numerical differentiation in Figure 1 yields -0.1.

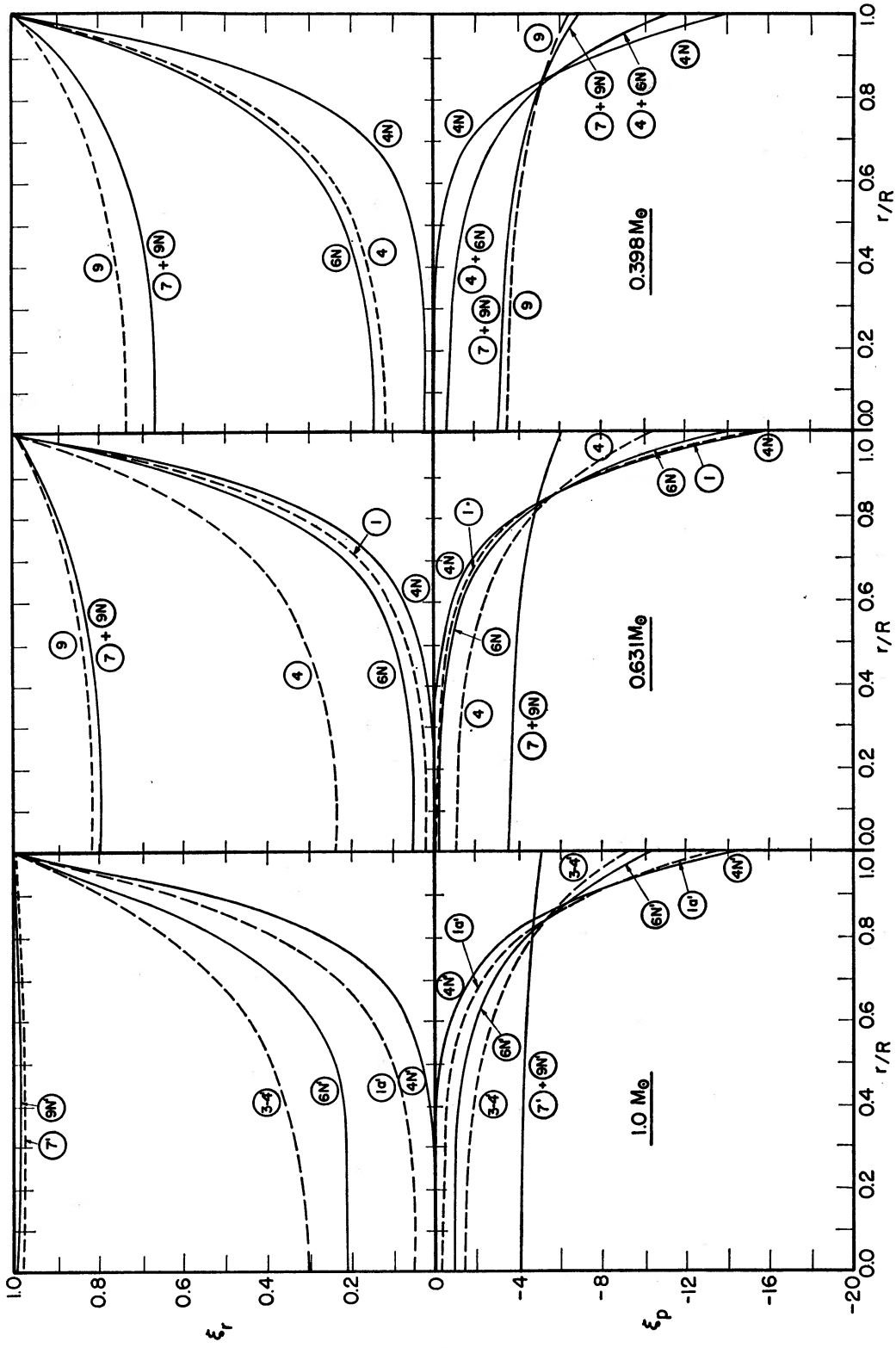

FIG. 4.—The fundamental-mode eigenfunctions ξ_r and ξ_p versus fractional radius. In each vertical section the upper and lower curves with the same model number give ξ_r and ξ_p, respectively, for the given model. Results are shown for both neutrino (*full curves*) and no-neutrino (*dashed curves*) models. Note the different scales for ξ_r and ξ_p.

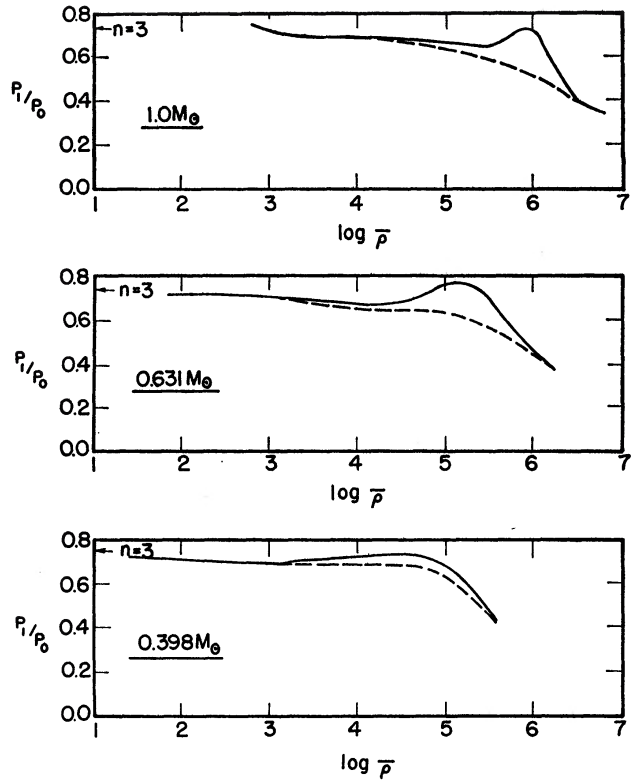

FIG. 5.—Variation with mean density and stellar mass of the ratio P_1/P_0 of first-harmonic to fundamental-mode pulsation periods. Both neutrino models (*full curves*) and no-neutrino models (*dashed curves*) are shown. The arrow marked $n = 3$ indicates the value for a polytrope of index $n = 3$.

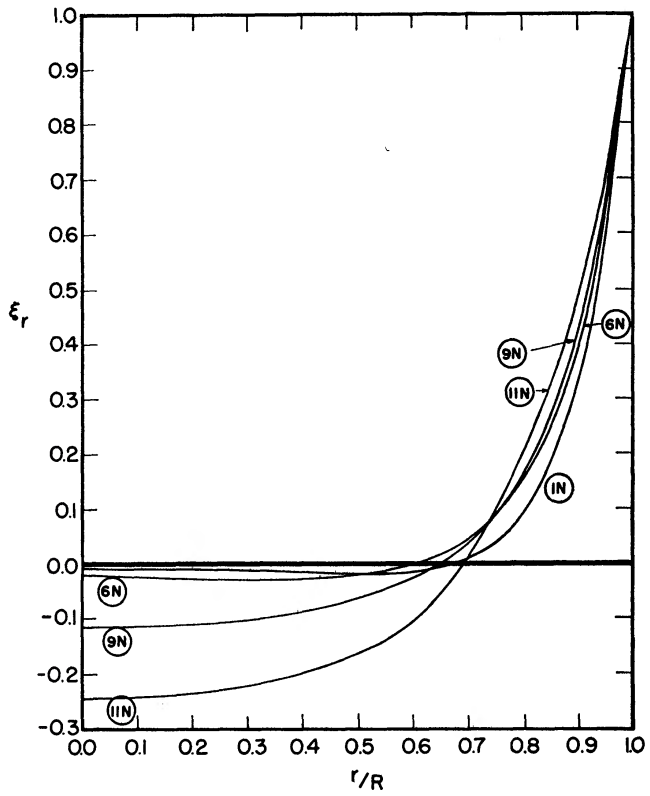

FIG. 6.—The first-harmonic, radial pulsation eigenfunction ξ_r for the 0.398 $M_\odot$ neutrino model sequence.

accuracy of these results is considerably less than for the lower modes. Of these results we quote only the ratio of periods of the first and second modes; our numerical calculations give

$$P_2/P_1 \approx 0.70 \pm 0.03 , \tag{14}$$

with no significant evidence for systematic variations with either neutrino emission or stellar mass.

The general trend of P_1/P_0 toward smaller values with increasing $\langle\rho\rangle$, as shown in Figure 5, is to be expected if our results are to be consistent with the results for an $n = 3$ polytrope ($P_1/P_0 = 0.738$ [Schwarzschild 1941; Hurley, Roberts, and Wright 1966]) in the limiting case of extreme nondegeneracy, and with the variational results for a white dwarf with a mass $\sim 1\ M_\odot$ ($P_1/P_0 = 0.610$ [Sauvenier-Goffin 1949]) in the opposite extreme. The difference between the results for the models with and without neutrino emission, however, requires further discussion of the factors that affect the overtone pulsation frequencies. This can be accomplished most directly by rewriting equation (3) for the eigenfrequency σ_m of the mth harmonic. An integration by parts, with Γ_1 assumed constant, gives

$$\sigma_m^2 = \int_0^R dr \frac{\xi_m^2 \rho r^4}{J_m} \left[\frac{\Gamma_1 p}{\rho} \frac{1}{H_m^2} + (3\Gamma_1 - 4) \frac{GM_r}{r^3} \right] , \tag{15}$$

where J_m is given by equation (4), and $H_m \equiv \xi_m/(d\xi_m/dr)$. Since ρ *increases* rapidly inward, while $\xi_m^2 r^4$ *decreases* inward, the normalized weight function $\xi_m^2 \rho r^4/J_m$ is very sharply peaked at some point $r = r_m$ in the outer envelope of the star. We may therefore approximate equation (15) by the bracketed terms, evaluated at $r = r_m$. Now we expect $R - r_m = \alpha H_m \ll R$, where α is of order unity. Since we also have, for a radiative envelope with a generalized Kramers's opacity law, $K = K_0 \rho^n T^{-s}$, the relation

$$\frac{p}{\rho} = \frac{kT}{\mu H} \approx \frac{n+1}{4+n+s} \frac{GM}{R^2} (R - r) , \tag{16}$$

we thus find for the period ratio

$$\frac{P_m^2}{P_{m-1}^2} = \frac{\sigma_{m-1}^2}{\sigma_m^2} = \frac{H_m(1+\epsilon_{m-1})}{H_{m-1}(1+\epsilon_m)} ; \quad \epsilon_m \equiv \frac{3\Gamma_1 - 4}{\Gamma_1} \frac{4+n+s}{\alpha(n+1)} \frac{H_m}{R} . \tag{17}$$

This equation contains the explanation for the systematic behavior of the P_1/P_0 ratio shown in Figure 5. Since the eigenfunction of the first overtone must *of necessity* decrease inward more rapidly than that of the fundamental, we have $H_1 < H_0 \ll R$, for the nondegenerate models, so that $P_1/P_0 \sim (H_1/H_0)^{1/2} < 1$. Furthermore, since H_0 increases more rapidly than H_1 as the stars become degenerate (see Figs. 4 and 6), we also expect P_1/P_0 to be smaller for the white-dwarf models than for the nondegenerate stars, as the numerical results show.

The systematic differences in behavior of the P_1/P_0 ratio between the neutrino and no-neutrino models can also be understood on the basis of equation (17). The copious neutrino emission in the latter models causes rapid contraction of the central core of the star, resulting in much larger $\rho_c/\langle\rho\rangle$ for a given $\langle\rho\rangle$ than in the no-neutrino models. By equation (12) and (13), however, this results in smaller values of Q^*, and therefore of H_m, for a star of given mean density; consequently, P_1/P_0 remains large to much larger values of $\langle\rho\rangle$ than in the no-neutrino stars.

This same sort of reasoning also shows why the ratio P_2/P_1 shows no appreciable systematic variation; the radial eigenfunctions of both the first and second overtones decrease so rapidly inward in *all* of the models (this is shown explicitly in Fig. 6 for the first-harmonic eigenfunctions) that the H_m's show little change as the stars become degenerate.

e) Stability Integrals

Our results for the stability integrals defined by equation (5) are listed in Tables 3–8 for the fundamental mode and in Table 10 for the first overtone of the 0.398 $M_\odot$ neutrino model. In addition, we have plotted in Figure 7 the running integral

$$\frac{1}{\kappa}\int_0^{M_r}\frac{d\kappa}{dM_r}\,dM_r$$

for the fundamental mode of each of the stellar models.

There are several interesting features of these curves. We first note that strong pulsational damping occurs in the stellar envelopes for r/R greater than, say, 0.7. This effect, which is typical of hot stars, is sufficient to guarantee stability for all models. For those models with neutrinos, the stability is further enhanced by the damping properties of the neutrino losses; i.e., the neutrino loss rates increase upon compression of the medium which tends to damp the pulsation.

A curious feature is exhibited by the highly evolved models without neutrino losses. In these cases the running integral of κ is either negative in the core of the model or shows a decrease from previously positive values as M_r increases. This indication of driving, due solely to radiative processes, is the result of the peculiar behavior of $\Gamma_3 = (d \ln T/d \ln \rho)_{ad} + 1$ in degenerate matter. At the center of the model, where the electron gas is strongly relativistically degenerate, Γ_3 is controlled by the ions and tends to be only slightly smaller than 5/3 (see, for example, the discussion in Hansen and Wheeler 1969). At somewhat larger values of M_r, however, the electron degeneracy is enough smaller so that the electron gas begins to affect Γ_3. Since the electrons are still relativistic in this region, Γ_3 thus decreases toward 4/3. When finally the region is reached where nonrelativistic, partial degeneracy occurs, Γ_3 again increases to a value near 5/3. In these dense models where the radial variation is nearly homologous, thus implying near homology also for the pressure variation, the effect of this dip in Γ_3 is to change the sign of the radial derivative of the temperature variation. Together with the small temperature gradient due to efficient electron conduction, this has the important effect of causing luminosity variations to change sign in the vicinity of the dip in Γ_3. The result is a transition from damping to driving or the converse, depending on the direction of the change in Γ_3. An interesting speculation is whether conditions could be found such that this effect could override both neutrino and envelope damping and result in instability.

Finally, it should be noted that, although the analysis leading to equation (5) for the damping integrals is adequate in most circumstances, there are clearly cases in which the present discussion is not entirely satisfactory. In the most degenerate models we have studied, the timescale of evolution of the star as measured by the e-folding time for the central temperature is shorter than the damping time κ^{-1} of the pulsations. The problem of determining the rate of growth or decay of the pulsations thus cannot be separated from the evolution of the star—in contrast to the normal situation in the study of pulsational instability. The effect of this coupling is difficult to estimate in advance, and it seems probable that only detailed numerical calculations can provide an answer.

V. SUMMARY

We have carried out a quantitative study of the pulsation properties of homogeneous stars, with no nuclear energy sources, which are in their final phases of evolution toward the white-dwarf stage. In particular, we have obtained numerical values for the quantities Q^*, P_1/P_0, P_2/P_1, ξ_r, ξ_p, and κ (or C_r) for several stages during the evolution. As the stars contract and become increasingly degenerate, the periods rapidly become shorter [since $Q^* = P_0(G\langle\rho\rangle)^{1/2} \approx$ constant], ranging from $P_0 \sim 10$ minutes for the least

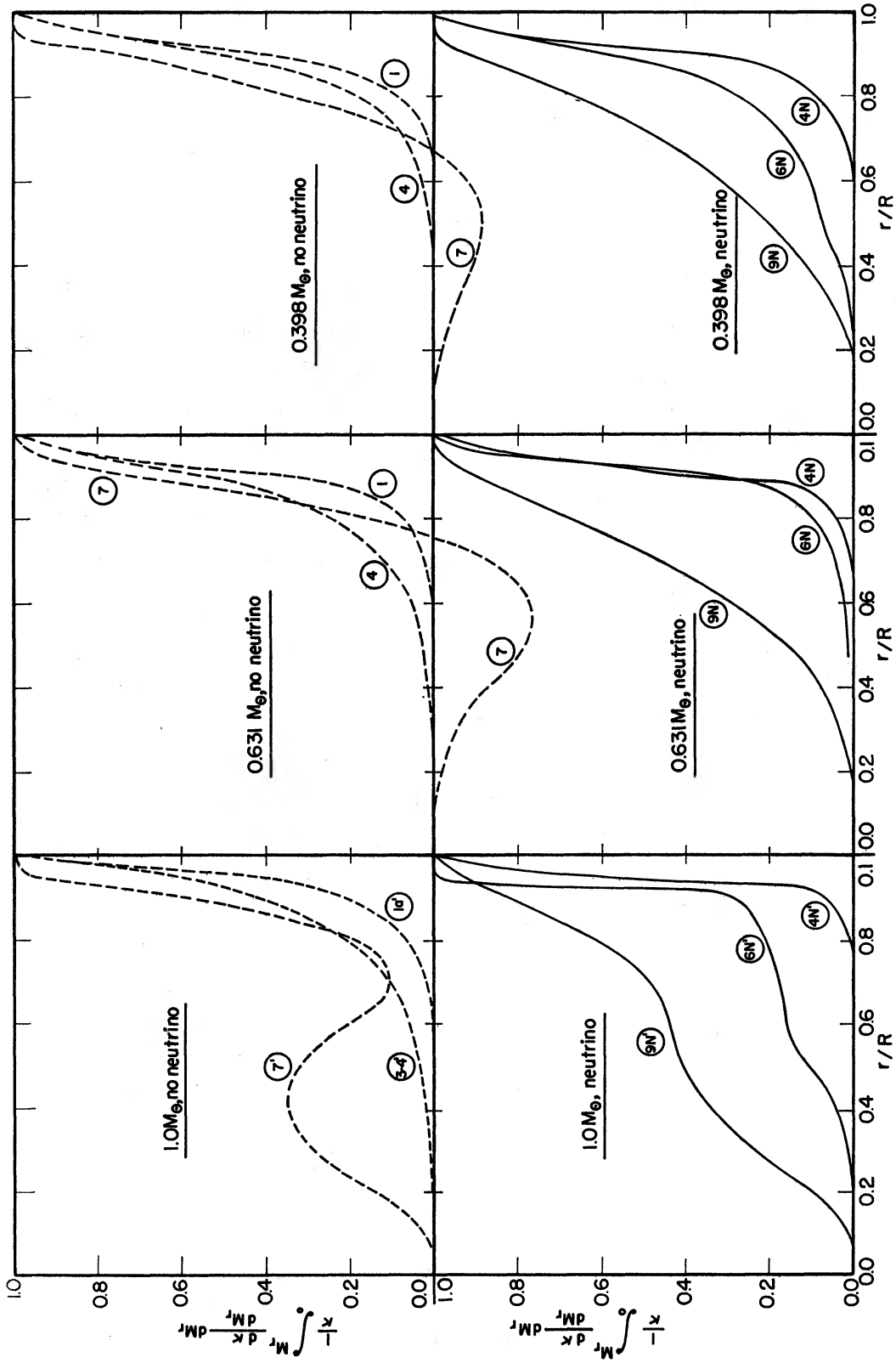

FIG. 7.—Variation with fractional radius of the accumulated damping integrals for both neutrino (*full curves*) and no-neutrino (*dashed curves*) sequences. Note that the damping integrals for the no-neutrino sequences are negative in part of the core of the more degenerate models, indicating that these regions are actually driving (see text).

degenerate models we considered to $P_0 \sim 10$ s for the white-dwarf configurations. Because of the extreme insensitivity of Q^* to changes in $\rho_c/\langle\rho\rangle$ in the early models, the constant-P_0 lines in the H-R diagram are almost completely unaffected by the neutrino processes. In a degenerate model, however, *all* of the model parameters are sensitive to changes in the internal structure of the star, and we have discussed this at some length in order to clarify the relation between changes in the structure of the unperturbed model and changes in at least some of the pulsational properties. In the limiting cases our results agree quite well (within our limits of error) with the results of previous calculations.

We have presented rather extensive numerical information about the pulsational properties of these homogeneous, pre–white-dwarf models, as well as detailed graphs of the eigenfunctions and stability integrals, since—to the best of our knowledge—such information has not previously been available for stars in these intermediate phases of evolution. It is our hope that these results may be of use in helping to understand the recently discovered ultrashort-period variable stars and that they may also provide a useful foundation for future work on the properties of stars below the main sequence.

We are grateful to Professors J. P. Cox and M. P. Savedoff for many helpful discussions. This work has been supported in part by the National Science Foundation under grants GP-13695 and GP-24944 through the University of Rochester and GP-12455 through the University of Colorado. Some of the computations were carried out at the Computing Center of the University of Rochester, which is in part supported by National Science Foundation grant GJ-828.

REFERENCES

Baglin, A. 1967, *Ann. d'ap.*, **30**, 617.
Bardeen, J. M., Thorne, K. S., and Meltzer, D. W. 1966, *Ap. J.*, **145**, 505.
Chandrasekhar, S. 1939, *Stellar Structure* (Chicago: University of Chicago Press), p. 412.
Cox, J. P., and Giuli, R. T. 1968, *Principles of Stellar Structure* (New York: Gordon & Breach).
Faulkner, J., and Gribbin, J. R. 1968, *Nature*, **218**, 734.
Gribbin, J. R., Feldman, P. A., and Plageman, S. H. 1970, *Nature*, **225**, 1123.
Hamada, T., and Salpeter, E. E. 1961, *Ap. J.*, **134**, 683.
Hansen, C. J., and Wheeler, J. C., 1969, *Ap. and Space Sci.*, **3**, 464.
Harper, R. Van R., and Rose, W. K. 1970, *Ap. J.*, **162**, 963.
Harrison, B. K., Thorne, K. S., Wakano, M., and Wheeler, J. A. 1965, *Gravitation Theory and Gravitational Collapse* (Chicago: University of Chicago Press).
Hurley, M., Roberts, P. H., and Wright, K. 1966, *Ap. J.*, **143**, 535.
Landolt, A. U. 1968, *Ap. J.*, **153**, 151.
Lasker, B. M., and Hesser, J. E. 1969, *Ap. J.* (*Letters*), **158**, L171.
———. 1971, *ibid.*, **163**, L89.
Ledoux, P., and Pekeris, C. L. 1941, *Ap. J.*, **94**, 124.
Ledoux, P., and Sauvenier-Goffin, E. 1950, *Ap. J.*, **111**, 611.
Ledoux, P., and Walraven, Th. 1958, *Hdb. d. Phys.*, **51**, 353.
Meltzer, D. W., and Thorne, K. S. 1966, *Ap. J.*, **145**, 514.
Ostriker, J. P., and Hesser, J. E. 1968, *Ap. J.* (*Letters*), **153**, L151.
Ostriker, J. P., and Tassoul, J. L. 1969, *Ap. J.*, **155**, 987.
Paczyński, B. 1970, *Acta Astr.*, **20**, 48.
Rose, W. K. 1967, *Ap. J.*, **150**, 193.
———. 1968, *ibid.*, **152**, 245.
Salpeter, E. E. 1961, *Ap. J.*, **134**, 669.
Sauvenier-Goffin, E. 1949, *Ann. d'ap.*, **12**, 39.
Savedoff, M. P., Van Horn, H. M., and Vila, S. C. 1969, *Ap. J.*, **155**, 221.
Schatzman, E. 1961, *Ann. d'ap.*, **24**, 237.
Schwarzschild, M. 1941, *Ap. J.*, **94**, 245.
Skilling, J. 1968, *Nature*, **218**, 923.
Van Horn, H. M., Cox, J. P., and Hansen, C. J. 1971, in preparation.
Vila, S. C. 1965, unpublished Ph.D. thesis, University of Rochester.
Walker, M. F. 1961, *Ap. J.*, **134**, 171.
Warner, B., and Nather, R. E. 1970, *M.N.R.A.S.*, **147**, 21.